14–40 MeV proton scattering from low-lying states of ^{28}Si

R. De Leo, G. D'Erasmo, A. Pantaleo, G. Pasquariello,* and G. Viesti*
Istituto di Fisica dell'Universitá, Bari-Italy, Istituto Nazionale di Fisica Nucleare, Sezione di Bari

M. Pignanelli
Istituto di Fisica dell'Universitá, Milano-Italy, Istituto Nazionale di Fisica Nucleare, Sezione di Milano

H. V. Geramb
Institut für Theor. Physik, Universität Hamburg, West Germany
(Received 12 January 1978; revised manuscript received 11 October 1978)

Differential cross sections for proton scattering from the six lowest states of ^{28}Si have been measured at 30 incident energies in the range 14–40 MeV. Differential spin-flip probabilities for proton scattering from ^{28}Si 2^+(1.78 MeV) state have been determined at ten incident energies in the range 16–22 MeV. Elastic data have been analyzed by means of the optical model. Compound nucleus contributions present at low energies in experimental data have been evaluated by means of the Hauser-Feshbach statistical model. Coupled-channels calculations and a macroscopic model have been used to analyze transitions to natural parity states. An anomalous behavior of the deduced deformation parameters has been obtained at low energies. The experimental data related to the 2^+ level and to the 3^+ unnatural parity state have been compared with the prediction of a microscopic antisymmetrized distorted wave calculation in which a direct reaction mechanism is supplemented by a two-step resonance contribution corresponding to the virtual excitation of giant resonance states of ^{28}Si. These contributions, essential to fully explain the data, have made the evaluation of the $E1$, $E2$, and $E3$ giant resonance strengths in ^{28}Si possible.

[NUCLEAR REACTIONS ^{28}Si$(p,p'\gamma)$, E_p = 14–40 MeV; measured $\sigma(E_p,\theta_{p'})$ for the six lowest states and $\sigma(E_p,\theta_{p'},\theta_\gamma=90°)$ for the first 2^+ level; deduced OM and deformation parameters and $E1$, $E2$, and $E3$ GR strengths of ^{28}Si. Natural targets.]

I. INTRODUCTION

Proton inelastic scattering from low-lying excited states of low-medium mass nuclei has for a long time been considered as a typical direct process. Recently it has been realized that, even at incident energies large enough to avoid sizeable compound nucleus contribution, features of the process such as excitation functions and angular distributions are not correctly described by direct reaction theories and that additional scattering mechanisms must be taken into account.[1-6]

As a consequence, semidirect effects and in particular two-step processes via a giant resonance (GR) have been introduced in the analyses of inelastic scattering experiments at medium incident energies.[1,4] The GR contributions normally yield cross sections with magnitude in the range of 0.1 to 1 mb/sr, which constitute a significant contribution to all inelastic channels.

In strong inelastic transitions, currently explained by macroscopic collective models, the contributions coming from GR can, for instance, manifest themselves in an energy dependence of the deformation parameters used in the calculation, or with discrepancies between calculated and experimental angular distributions.[5] The difficulty of having to unfold direct and semidirect contributions is offset in the case of inelastic transitions to states having non-normal spin-parity combinations, since the direct excitation of these states is strongly hindered.[1,4,6] In this case the study of inelastic scattering to low-lying states may constitute a valid way to explore the properties of the intermediate state, which for appropriate choices of the incident energy can be identified as a giant resonance.

In this work we investigate the inelastic scattering of protons from ^{28}Si for transitions to low-lying states up to 7 MeV of excitation at incident energies between 14 and 40 MeV. Our aim is to make evident the importance of two-step processes and possibly to deduce the strength distribution of GR excited in the intermediate state. Valid tools to this end are represented by spin dependent data, owing to their sensitivity to reaction mechanism details.[1] Such data are given in the present experiment by the proton spin-flip probability (SFP) in the scattering from the first 2^+ (1.78 MeV) level and by the cross section for the unnatural parity state 3^+ (6.27 MeV) since both data require a spin momentum transfer $\Delta S = 1$ by the incoming proton.

Following the predictions of collective models the chosen energy interval should contain GR cen-

troids of different multipolarities. The giant dipole resonance (GDR) of ^{28}Si has been clearly evidenced by photonuclear reactions[7]; however, a large indeterminacy still exists for other GR multipolarities. The giant quadrupole resonance (GQR), whose centroid is predicted at about 20 MeV, at present seems to be spread out from 15 to 30 MeV, as indicated by the bumps in the continuous spectra of the inelastically scattered α particles.[8]

In Sec. II the details of the experiment are given, while the result of our optical model analysis of the elastic scattering, of compound nucleus contribution evaluation and macroscopic model prediction for 2^+, 4^+, and 3^- levels are reported, respectively, in Secs. III, IV, and V. Section VI is devoted to the analysis of the data relative to the transitions to 2^+ and 3^+ states with a microscopic distorted-wave Born approximation (DWBA) supplemented by the inclusion of a two-step mechanism. The conclusions are summarized in Sec. VII.

II. THE EXPERIMENTAL METHOD AND RESULTS

The analyzed proton beam from the Milan AVF cyclotron was focussed onto a target at the center of a 60 cm diameter scattering chamber. Natural

TABLE I. Optical model parameters of ^{28}Si. The potentials listed are of the form $U(r) = -Vf(x_v) + i4W_D(d/dx_W)f(x_W) - Wf(x_W) - (\hbar/m_\pi c)^2 \frac{1}{2} V_{so} f(x_{so}) + V_c$, where $f(x_i)$ is a Saxon–Woods form factor, $x_i = (r - r_i A^{1/3})$ and V_c is the Coulomb potential of a uniformly charged sphere of radius $R = 1.2A^{1/3}$ fm. The following geometrical parameters have been used: $r_v = 1.17$, $a_v = 0.673$, $r_w = 1.33$, $a_w = 0.575$, $r_{so} = 1.07$, and $a_{so} = 0.78$ fm.

Set	E_p (MeV)	V (MeV)	W (MeV)	W_D (MeV)	V_{so} (MeV)	χ_1^2 [b]	χ_2^2 [b]
1	14.26	55.5	4.47	1.61	5.65	6.2	13.0
	15.34	45.9	4.94	1.80	5.97	2.5	10.1
	15.83	54.2	8.63	0.0	6.97	4.2	16.0
	16.30	50.5	2.88	5.11	5.79	3.0	10.5
	16.80	49.5	6.95	1.12	5.81	1.9	9.1
	17.24	48.7	4.43	2.91	7.49	5.2	10.0
	17.67	48.6	5.74	1.33	7.61	1.2	9.1
	18.18	49.7	3.15	4.33	6.94	1.2	3.5
	18.73	48.3	2.63	4.11	8.77	1.2	5.0
	19.27	49.1	4.00	3.77	7.86	1.1	5.0
	19.70	48.1	1.70	5.00	6.54	1.8	2.2
	20.17	47.7	0.96	5.41	6.21	1.8	2.1
	21.32	46.9	0.0	6.29	5.08	4.6	6.6
	22.70	48.0	0.0	6.04	6.01	4.1	4.1
	23.60	46.6	1.16	4.91	5.34	1.4	5.6
	24.24	48.5	0.12	6.35	9.15	4.8	5.5
	25.44	47.8	0.25	5.77	8.49	2.3	5.1
	26.34	46.5	0.0	5.69	8.71	2.5	6.7
	27.30	46.6	0.39	5.57	7.99	2.9	4.5
	28.70	45.3	1.87	4.42	7.58	2.9	3.3
	29.47	45.2	1.76	4.28	7.00	1.9	1.9
	30.5	44.6	2.24	3.81	6.49	2.1	2.0
	31.50	44.7	2.73	3.60	5.96	1.2	1.1
	32.40	45.0	3.55	3.16	5.45	0.9	1.0
	33.70	45.1	4.06	2.89	5.47	0.7	1.0
	34.70	44.4	4.61	2.56	5.58	0.7	1.0
	35.97	43.5	4.62	2.36	5.41	0.7	1.1
	37.21	42.6	4.58	2.22	5.42	1.1	2.2
	38.60	42.9	3.71	2.65	5.14	1.5	3.8
	40.21	43.0	4.89	2.17	4.88	1.8	7.9
2	E 5.9–0.32E		11.8–0.25E [a]		6.0	2.27	5.3
		0.32E–8.0					

[a] At energies lower than 22 MeV the value $W_D = 6.3$ was used.

[b] The χ^2 values given in the Table have been calculated assuming a 10% constant error of the experimental points. The number listed as χ_1^2 are χ^2 values obtained by searching on potential depths, while χ_2^2 have been obtained by using the average set 2 at each incident energy.

Si targets were used owing to the high and well known ^{28}Si content. In a first set of measurements a 4.47 mg/cm^2 thick target was used. Differential cross sections were measured at the 30 incident energies listed in Table I for the transitions to the following final states: g.s. (0^+), 1.78 MeV (2^+), 4.62 MeV (4^+), 4.98 MeV (0_2^+), 6.28 MeV (3^+), and the unresolved doublet 6.88 MeV (3^-) – 6.89 MeV (4^+). In a second set of measurements the spin-flip probabilities for the transition to the first 2^+ excited state were obtained by counting protons in coincidence with the deexcitation γ rays emitted perpendicularly to the scattering plane. The SFP were measured at the following incident energies: 16.30, 17.24, 17.67, 18.18, 18.73, 19.23, 19.70, 20.17, 21.35, and 22.70 MeV. In the latter experiment a 11.2 mg/cm^2 thick target was used. The energy loss in the target was taken into account in both experiments in determining the average effective incident energy.

The scattered protons were detected by 3 counters made up by totally depleted surface barrier detectors; measurements requiring thicknesses larger than 5 mm were performed by stacking two or three transmission detectors. Proton counters were mounted on a movable plate inside the scattering chamber. γ rays were detected by means of a 5 cm×5 cm NaI (Tl) cylindrical crystal positioned 30 cm away from the target outside the scattering chamber. The angular resolution was 2°–3° and 4°, respectively for proton and γ detectors. Typical spectra for thin and thick targets are given in Fig. 1.

A more detailed description of the experimental apparatus, data collection and reduction, especially for what concerns SFP measurements, has been reported elsewhere.[5]

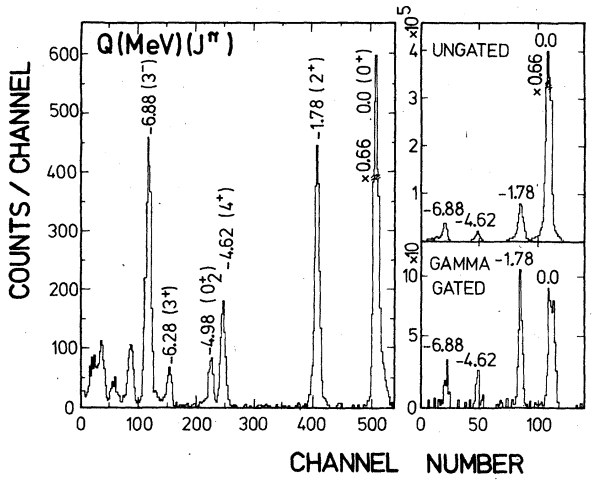

FIG. 1. Example of proton spectra for thin (left side) and thick (right side) ^{28}Si target taken at E_p = 33.7 MeV, θ_{lab} = 45° and at E_p = 18.73 MeV, θ_{lab} = 27°, respectively.

The experimental errors affecting our data are indicated in the figures for only SFP measurements and they essentially represent statistical indeterminacy. Cross section overall uncertainties are 5% except for the 3^+ and 0_2^+ levels where the statistical errors and the background subtraction process increase this value to 10% and 15%, respectively.

III. OPTICAL MODEL ANALYSIS OF ELASTIC SCATTERING DATA

As direct reaction models generally use distorted waves for the incoming and outgoing channels, optical model (OM) potentials are needed for all the energies investigated in this work.

Recently it has been ascertained that elastic scattering from medium-light nuclei at these energies suffers from resonant effects.[6,9,10] In previous analyses,[2,9] to avoid resonance influence in deriving OM parameters, experimental cross section data were employed only at forward angles. For ^{28}Si, proton elastic scattering data between 15° and 55° were found[2] still affected by an energy dependence between 17 and 29 MeV. This evidence induced us to consider the whole angular distribution; so to avoid resonant effects, we searched for OM parameters with constant geometries at all measured energies and with regular energy well depth behaviors.

The computer code MERCY,[11] including a least squares routine and a standard OM potential of the form given in Table I, was used. For a better determination of the spin-orbit term the published data on polarization[10] at 20.3, 25.25, and 30.5 were also considered.

The energy independent OM geometry, reported in the footnote (a) of Table I, causing the overall minimum χ^2, was obtained by a multistep grid imposed on each geometric parameter and by leaving the potential depths free to vary. This geometry caused the well depth values reported as set 1 in Table I; the fits obtained are displayed, at some energies only, in Fig. 2 with dashed lines, while the relative χ^2 are reported as χ_1^2 in Table I. The fit agreement results better at forward angles and at higher energies where nondirect effects are expected to be negligible in respect to direct contributions.

The well depth fluctuations observed in the set 1 are not confined to a particular parameter and energy region as previous works[6,9,12] have found but appear numerous, of small entity, and uncorrelated among themselves; consequently the energy averaged OM depth set, labeled 2 in Table I, was

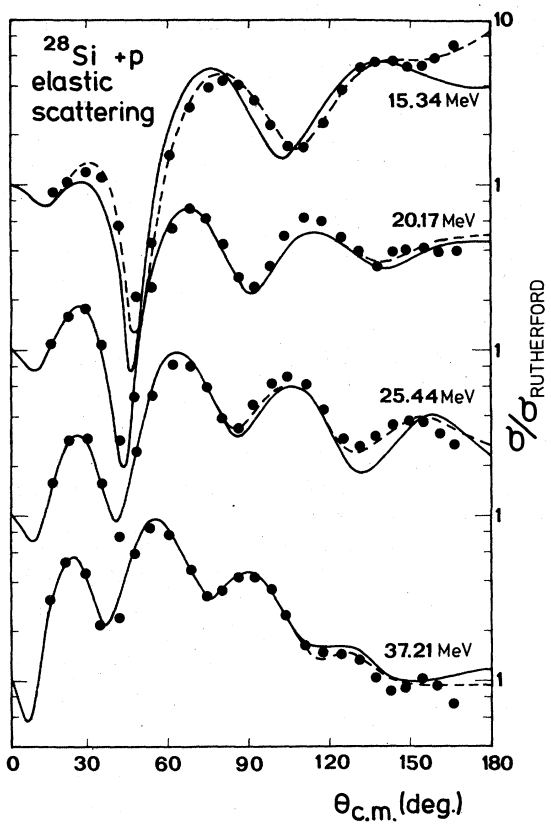

FIG. 2. Proton elastic cross section data together with OM fits obtained using parameters in Table I (set 1 dashed lines, set 2 full lines).

obtained by averaging set 1 depths with a constant value for the spin-orbit term and with a linear energy dependence for the real and imaginary depths. Except for a few cases in the low energy region the fits (full lines in Fig. 2) and the χ^2 (χ_2^2 in Table I) result very close to those of set 1.

It must be noted that the potential labeled set 2 presents geometries and energy dependences very similar to those found by Becchetti and Greenlees[13] for heavier nuclei.

V. EVALUATION OF COMPOUND NUCLEUS CONTRIBUTIONS

A wide interval of incident energies has been investigated in this work to find out the range in which two-step processes are relevant. As regards the lowest limit, measurements below 14 MeV are senseless due to the closing of many reaction channels and to the consequent dominant presence of compound nucleus (CN) contributions. These contributions might be, however, not negligible also above 14 MeV.

^{28}Si(p,p') excitation functions have been measured by Kemper *et al.*[14] between 16 and 18 MeV and by Shotter *et al.*[15] between 12 and 15 MeV. Correlated fluctuations with widths of 300 keV, not interpretable in terms of Ericson statistical fluctuations,[16] have been found in many (p,p') transitions, indicating the presence of both CN and door-way state contributions in the reaction mechanism.

In absence of any quantitative determination of door-way state contributions, the CN evaluated cross sections, summed up with direct contributions, are expected to be always lower than the experimental points averaged over an appropriate energy interval to smooth out Ericson fluctuations.

CN contributions have been evaluated using the Hauser-Feshbach (HF) statistical model.[17] The (p,p'), (p,n), (p,d), and (p,α) channels have been considered in the CN decay. The OM parameters used to describe the channels considered are given in Table II. The proton potential, taken from Sec. III, reproduces the experimental total reaction cross sections[20] within 5%. The level densities for residual nuclei have been evaluated using the Fermi-gas model formula[21] with the back shift of Ref. 22 for the energy scale; the pairing energies have been taken from Ref. 23.

Calculated elastic and inelastic cross sections along with experimental data are shown in Figs. 3 and 4. The calculations for the inelastic scattering include collective DWBA contributions with deformation parameters obtained from the higher energy data (see Sec. V) in addition to the HF calculation. Because of uncertainties in the parameters used

TABLE II. Optical model parameters used to evaluate compound nucleus contributions.

Channel	V	r_v	a_v	W_D	r_w	a_w	V_{so}[a]	r_c	Ref.
neutron	$47.01-0.267E-0.0018E^2$	1.3	0.66	$9.52-0.053E$	1.257	0.48	7.00[b]	•••	18
proton	$54.9-0.32E$	1.17	0.673	6.3	1.33	0.6	5.4	1.2	present work
alpha	190.8	1.43	0.608	9.91	1.78	0.39	0.0	1.4	18
deuteron	101.3	1.05	0.86	23.6	1.43	0.62	7.0	1.3	18

[a] r_{so} and a_{so} fixed at r_v and a_v values, respectively.
[b] Estimated from Ref. 19.

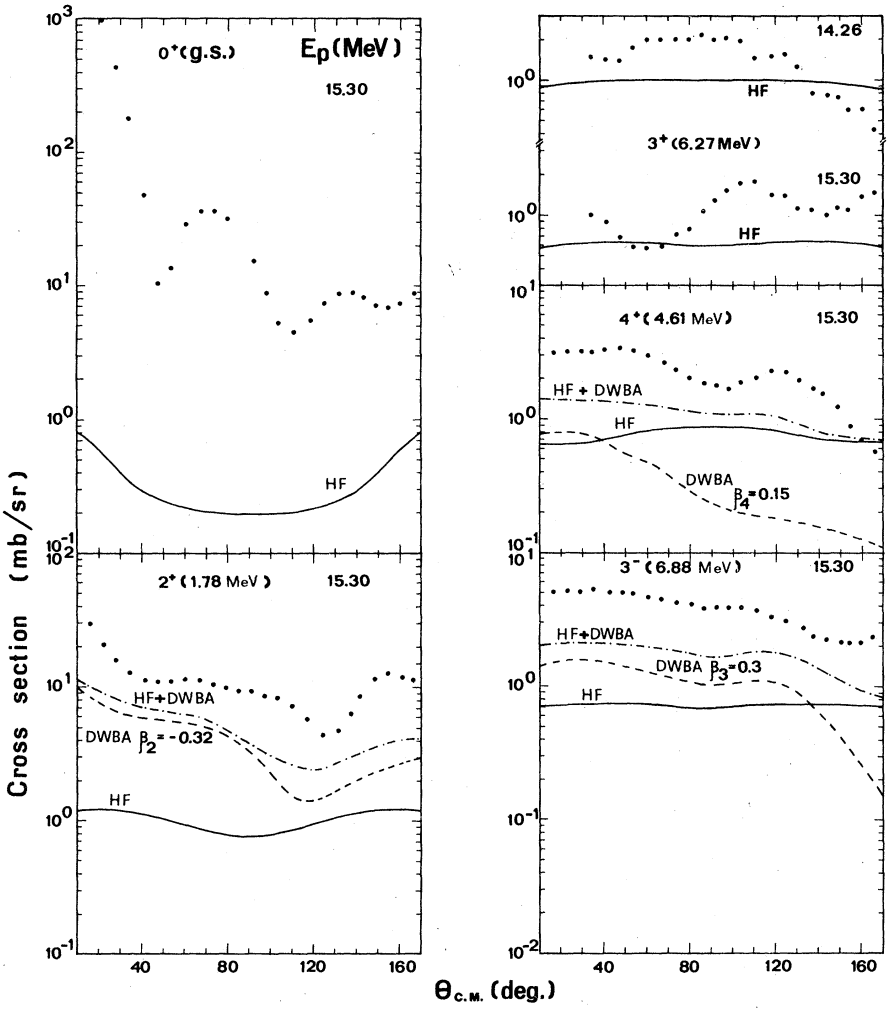

FIG. 3. Differential cross sections (points) for the reaction ^{28}Si(p,p') on various excited levels. Curves labeled HF represent the compound nucleus contribution as evaluated by the HF program; the DWBA curves represent the direct reaction contribution evaluated with OM parameters from set 2 of Table I and deformation parameters taken from Fig. 12 averaging values at high incident proton energies. Point-dashed lines represent the sum of the two contributions.

in the latter calculation, one cannot rely on the accuracy of the magnitude of the CN estimate. Since in some cases the sum of CN and DWBA calculations exceeds the data, in particular it exceeds the ones of Ref. 15 averaged over an interval of 500 keV (Fig. 4), we have arbitrarily reduced the CN contribution by the factor $\frac{2}{3}$. The resulting cross sections have then been simply subtracted from the data. Owing to the rapid energy dependence of statistical effects, CN contributions are significant only below 17 MeV and for transitions to high angular momentum states.

V. MACROSCOPIC INTERPRETATION OF NATURAL PARITY TRANSITIONS

In this section the experimental data, with the exception of those concerning the 3^+ and 0^+_2 states, are analyzed with a direct reaction mechanism and a collective description of the nucleus. The principal aim is to evidence nondirect processes by means of the anomalous energy dependence of some parameters used in the calculation.

The coupled channel (CC) program ECIS by Raynal[24] including a search routine on OM parameters and deformations, has been used. This program contains the full Thomas form for the spin-orbit deformation[25] and permits the spin-orbit and central potentials to be deformed in a separate way by using different deformation parameters (β^{so}, β^{cent}, respectively).

Several runs of the program performed on the $K^\pi = 0^+$ rotational band ascertained that (a) in CC calculations, the imaginary term of OM potentials deduced from elastic data analysis must be decreased of 0.5 MeV since it no longer accounts for some inelastic channels, (b) no appreciable difference is evident in the fits or in the deformation parameters deduced using the two sets of OM pa-

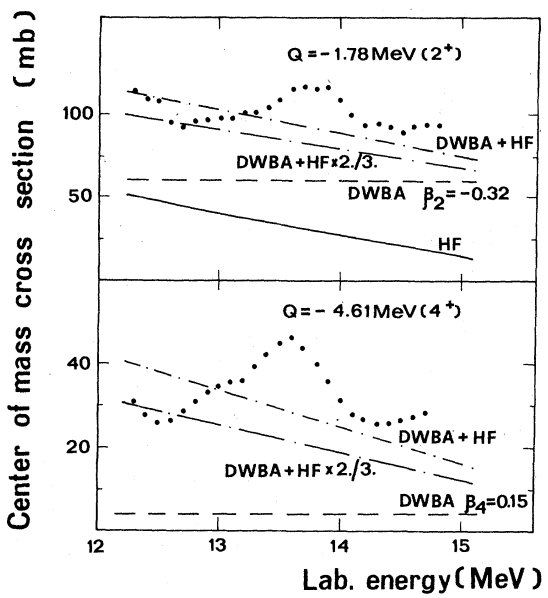

FIG. 4. Integral cross sections averaged over an incident proton energy interval of 500 KeV (points) for the reaction ^{28}Si(p,p') on the two excited levels quoted. The curves have the same meaning of the ones in Fig. 3; moreover an additional point-dashed line has been drawn in which only the $\frac{2}{3}$ of the estimated HF contribution has been added to the direct one.

rameters of Table I, (c) SFP data, shown in Fig. 5 together with measurements at 29.7 and 40.0 MeV taken from Ref. 26, are very sensitive, both in shape and in absolute value, to the ratio $\beta_2^{so}/\beta_2^{cent}$ (see curves drawn in Fig. 5), and quite insensitive to their absolute values.

Some results of a three parameter (W_D, β_2, β_4) fit are displayed in Fig. 6. In these fits the constraint $\beta^{cent}=\beta^{so}$ has been used. The values obtained for the free parameters are marked with points in Fig. 7, where the bars attached to β values represent correlation errors, related to the number of fit free parameters and to their interdependence.

Values obtained for β_2 and β_4 are energy dependent; in fact, at low energies, they show an enhancement, particularly large for β_4. The subtraction from experimental data of CN contributions modifies β values at low energies; however, while this correction accounts for most of the β_2 enhancement, it does not restore the β_4 values found between 30 and 40 MeV. This happens also when the reduction of the factor $\frac{2}{3}$, imposed on statistical contributions in Sec. IV, is disregarded. The β values obtained at high energies are in good agreement with previous evaluation.[10,27] The β_4 increase at low energies may be interpreted as an estimate of nondirect contributions.

The experimental data of the doublet ($3^-, 4^+$) have been analyzed assuming a dominant 3^- contribution. In fact a hexadecapole deformation with a reasonable β_4 value, for example 0.15, accounts for only a small percentage of the experimental data. The results of this analysis are shown in Fig. 6 at only some energies, while the extracted β_3 values are reported in Fig. 7. The β_3 behavior is similar to the β_4 one also for what concerns the subtraction of CN contributions.

It must be noted that in the above analysis, the resonance or nondirect effect height has been completely parametrized in terms of β value increments. These increments have been found very large for β_3 and β_4 and less evident for β_2; they definitely vanish at energies greater than 26 MeV where, however, good fits have been obtained for the 2^+ angular distributions only. Above 26 MeV and at large angles, discrepancies between experimental and evaluated data do exist both for the 2^+ spin-dependent data and for the other cross sections.

Thus nondirect effects are evident in all the inelastic data influencing the 14–26 and 26–40 MeV ranges to different extents. In particular, below 26 MeV, all angular distributions are influenced both in shape and in absolute value, while, with the exception of the 2^+ cross sections, at larger energies only their shapes are modified.

VI. MICROSCOPIC ANALYSIS AND EXCHANGE PROCESSES

In case of transitions to non-natural parity states, where the direct process is lowered by angular momentum-parity conservation rules, one expects relatively large contributions coming from two-step processes. In fact, as a spin-flip ($\Delta S=1$) is required, only a part of the nucleon-nucleon interaction can act in the process.

It has recently been shown that other spin dependent data, such as asymmetries and SFP associated with the excitation of natural parity states, can constitute an excellent tool to study semidirect processes.[4,5]

In this section the data relative to the 2^+ and 3^+ levels are analyzed with MEPHISTO ,[1] a code for a microscopic antisymmetrized distorted wave calculation, in which the direct reaction mechanism is supplemented by a two-step contribution associated with the excitation of GR. As a detailed description of this calculation has been published elsewhere,[1,4] only relevant features are reported here.

The amplitude for inelastic scattering is given as a coherent sum of single particle amplitudes:

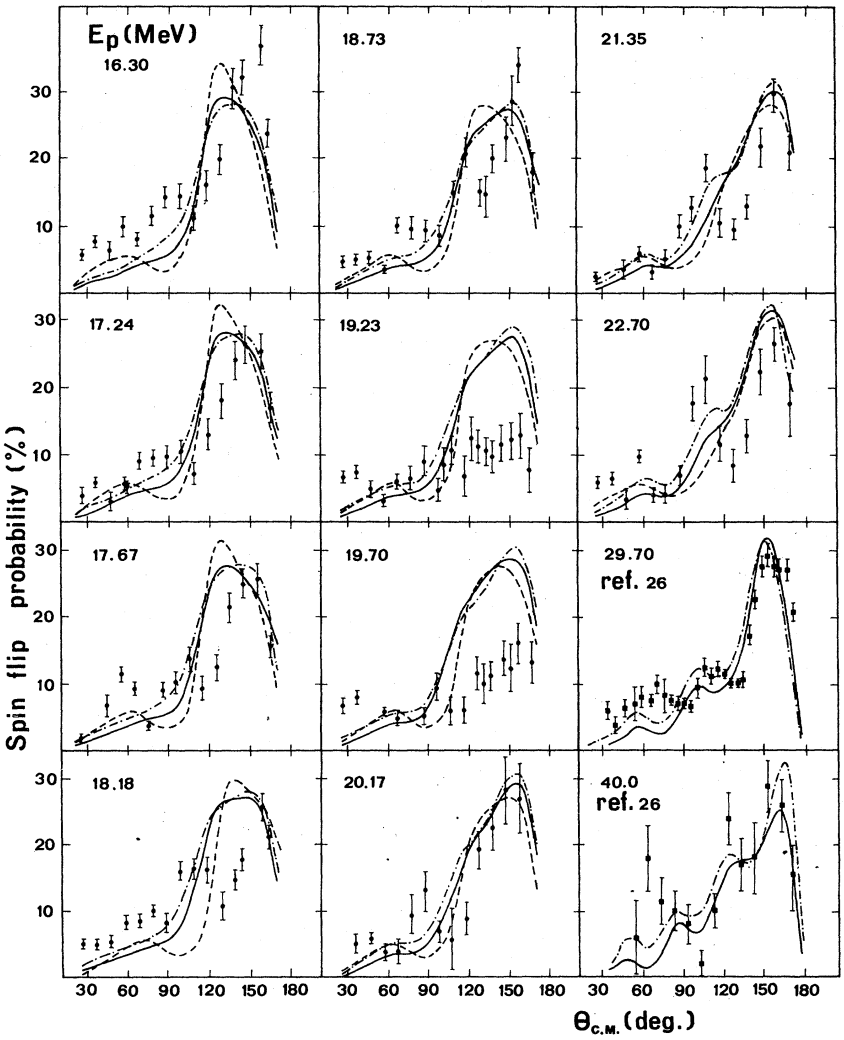

FIG. 5. Spin-flip probability for the inelastic proton scattering from the 2^+ level of ^{28}Si. The curves represent the results of a CC calculation obtained with $\beta_2^{cent} = -0.32$ and with OM parameters taken from set 2 of Table I. The influence of the ratio $\beta_2^{so}/\beta_2^{cent}$ on the calculation is shown (the ratio is equal to 0, 1.0, and 1.5 for dashed, continuous and point-dashed lines, respectively).

$$T_{sp} = \langle \chi_f^-(0)\phi_{j_2}(1)|t(0,1)|\chi_i^+(0)\phi_{j_1}(1) - \chi_i^+(1)\phi_{j_1}(0)\rangle - \Sigma_{\lambda\mu} M_\lambda(\bar{Q})\langle \chi_f^-(0)|V_{\lambda\mu}(0)|\phi_{j_1}(0)\rangle \times \langle \phi_{j_2}(1)|V_{\lambda\mu}(1)|\chi_i^+(1)\rangle , \quad (6.1)$$

where $\chi^\pm$ are distorted waves described by optical model wave functions (set 2 of Table I has been used). The bound states orbitals ϕ_{j_1}, ϕ_{j_2} are harmonic oscillator states with an oscillator strength fixed at 10.6 MeV. The number of single particle transitions $(j_1 \to j_2)$ is specified by the spectroscopy assumed for the considered $(J_i \to J_f)$ process. For both neutron and proton orbits each transition is weighted by its spectroscopic amplitude[28]:

$$S(j_1, j_2, J_i, J_f, I) = \langle J_f \| \{a_{j_2}^\dagger a_{j_1}\}^I \| J_i \rangle .$$

In the previous formula I is the total angular momentum transferred and a_{j_1}, $a_{j_2}^\dagger$ are destruction and creation operators. Spectroscopic amplitudes for analyzed transitions have been obtained from a recent evaluation by Wildenthal[29] (Table III).

The interaction operator $t(0,1)$ can be given as the sum: $V(0,1) + V_{CPD}(0,1)$. The first term represents an effective nucleon-nucleon interaction and is given as a mixture of central, tensor, and spin-orbit components, each with a Gaussian type[30] finite range form factor. For the central part, this interaction is equivalent to the long range part of the Hamada-Johnston potential. The noncentral components are based on the Eikemaier and Hackenbroich[31] force. Only the strength of the spin-orbit term, V_{LS}, has not yet been well established, so it is often empirically adjusted. The term $V(0,1)$ averaged over the appropriate wave functions and weighed by the assumed spectroscopic factors, gives the one-step process originated by transitions of valence nucleons.

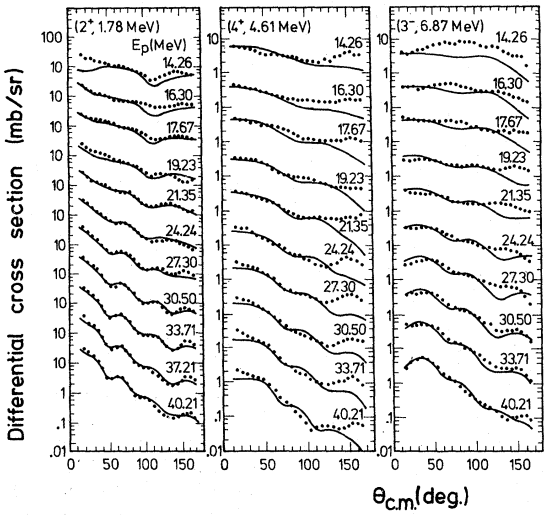

FIG. 6. Differential cross sections for the inelastic proton scattering from the 2^+, 4^+, and 3^- states of ^{28}Si at the energies quoted. The curves represent the result of a CC calculation obtained with the OM parameters taken from set 2 of Table I and with deformation parameters from Fig. 7.

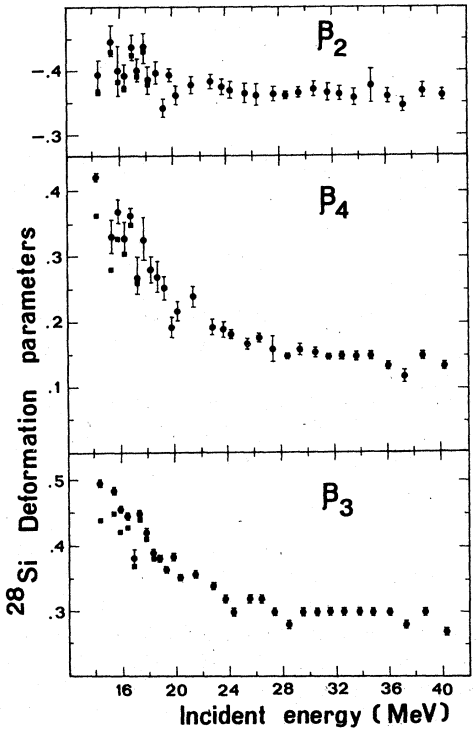

FIG. 7. Energy dependence of the quadrupolar, octupolar, and hexadecapolar deformation parameters evaluated with CC calculations. The squares give the values corrected by subtracting CN contributions.

TABLE III. Spectroscopic amplitudes for the 0^+-2^+ (1.78 MeV) and 0^+-3^+ (6.28 MeV) transitions in ^{28}Si.

$n_1l_1j_1, n_2l_2j_2$		0^+-2^+	0^+-3^+
$1d_{5/2}$	$1d_{5/2}$	0.4943	0.0298
$1d_{5/2}$	$2s_{1/2}$	0.9325	−0.5728
$1d_{5/2}$	$1d_{3/2}$	−0.5907	0.3619
$2s_{1/2}$	$1d_{5/2}$	0.6383	0.1366
$2s_{1/2}$	$1d_{3/2}$	−0.2484	...
$1d_{3/2}$	$1d_{5/2}$	0.4867	−0.0011
$1d_{3/2}$	$2s_{1/2}$	0.1437	...
$1d_{3/2}$	$1d_{3/2}$	0.3093	0.1019

The $V_{CPD}(0,1)$ term corresponds to the direct core polarization, accounting for the contributions omitted in the evaluation of valence transitions. The selection rules on spin, isospin, and angular momentum[32] cancel the core direct polarization term when a spin-flip occurs, as in the excitation

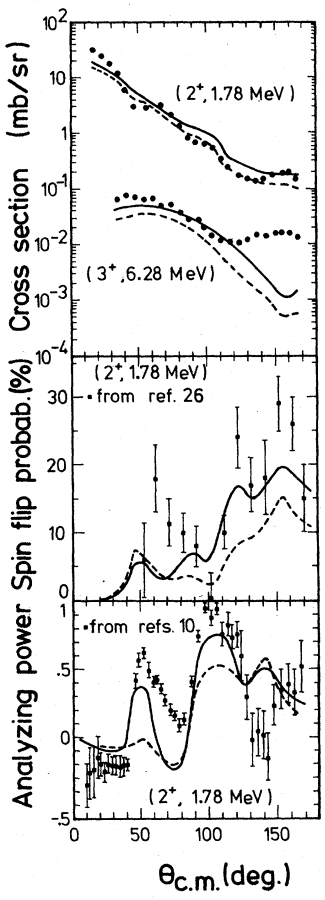

FIG. 8. Experimental angular distributions for the 2^+ and 3^+ transitions at $E_p = 40.0$ MeV. The curves represent the results of the total valence plus the direct core part of a microscopic calculation performed with the LS two body force strength fixed at 0.5 (full lines) and at 0.25 (dashed lines).

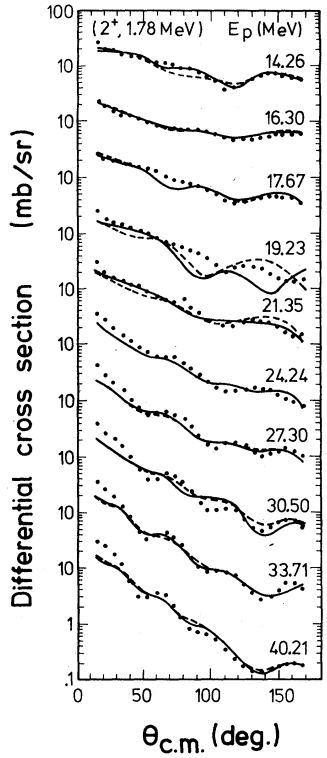

FIG. 9. Differential cross sections for the inelastic proton scattering to the 2^+ state of ^{28}Si. The curves represent the results of the microscopic ADWBA calculation in which the valence and core, direct, and exchange parts have been included. The full lines refer to the inclusion of three intermediate resonances with multipolarities $\lambda=1,2,3$ in the core exchange part and with complex strengths shown in Fig. 13. The dashed lines refer to two multipolarities $\lambda=1,2$ only.

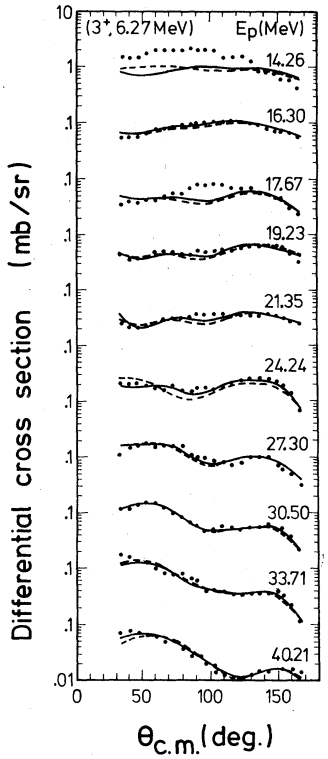

FIG. 10. As Fig. 9 for the 3^+ state of ^{28}Si. Relative complex strengths for the core exchange part are shown in Fig. 14 for the three multipolarity search.

of the non-natural parity state 3^+, and restrict the contribution to only the quadrupole term in a $0^+ - 2^+$ excitation. In such a case the coupling strength of the core direct polarization is fixed from the polarization charge required by the spectroscopy used to give the experimental $B(E2)$ value. The Wildenthal wave functions for ^{28}Si exact a polarization charge $e_{\rm pol}=0.5e$, accounting for an experimental $B(E2)$ value of 66 e^2 fm^4.

The approach, outlined in Ref. 4, requires multipole form factors, whose normalization is determined by coupling parameters $Y_L(Q)$. For the $0^+ \rightarrow 2^+$ transition and polarization charge 0.5 e, the coupling parameter $Y_2^{\rm CPD}$ proves to be equal to 0.0023 MeV^{-1}.

The second part of Eq. (6.1) describes the two-step resonance contribution. The amplitude represents a process whereby the projectile is captured by the target into a bound orbital (ϕ_{j_2}) transferring energy, momentum, and isospin to the nucleus. In the second step the nucleus deexcites itself transferring energy, momentum, spin, and isospin to one of the valence nucleons and ejecting it into the continuum.

To evaluate the two-step resonance amplitudes a collective model representation is used. Each multipole in the sum of Eq. (6.1) is identified as a giant resonance of centroid energy $\hbar w_\lambda$ and of width Γ_λ. In principle all multipoles can contribute to the process, each with a complex coupling constant[1]:

$$M_\lambda(\overline{Q}) = Y_\lambda(\overline{Q})e^{i\phi_\lambda(\overline{Q})}$$
$$= -\frac{\beta_\lambda^{\,2}}{2\lambda+1}\,(\overline{Q}-\hbar w_\lambda+\tfrac{1}{2}i\Gamma_\lambda)^{-1}. \qquad (6.2)$$

$\overline{Q}$ is the sum of the projectile energy and of the spectator binding energy: $\overline{Q}=E_p(cm)-\epsilon_{j_2}$; β_λ is the usual collective model deformation parameter measuring the total transition strength to form the GR of multipolarity λ from the ground state. In our version the calculation does not depend on the isospin of the resonances. The values allowed for β_λ are constrained by the energy weighted sum rules[33]

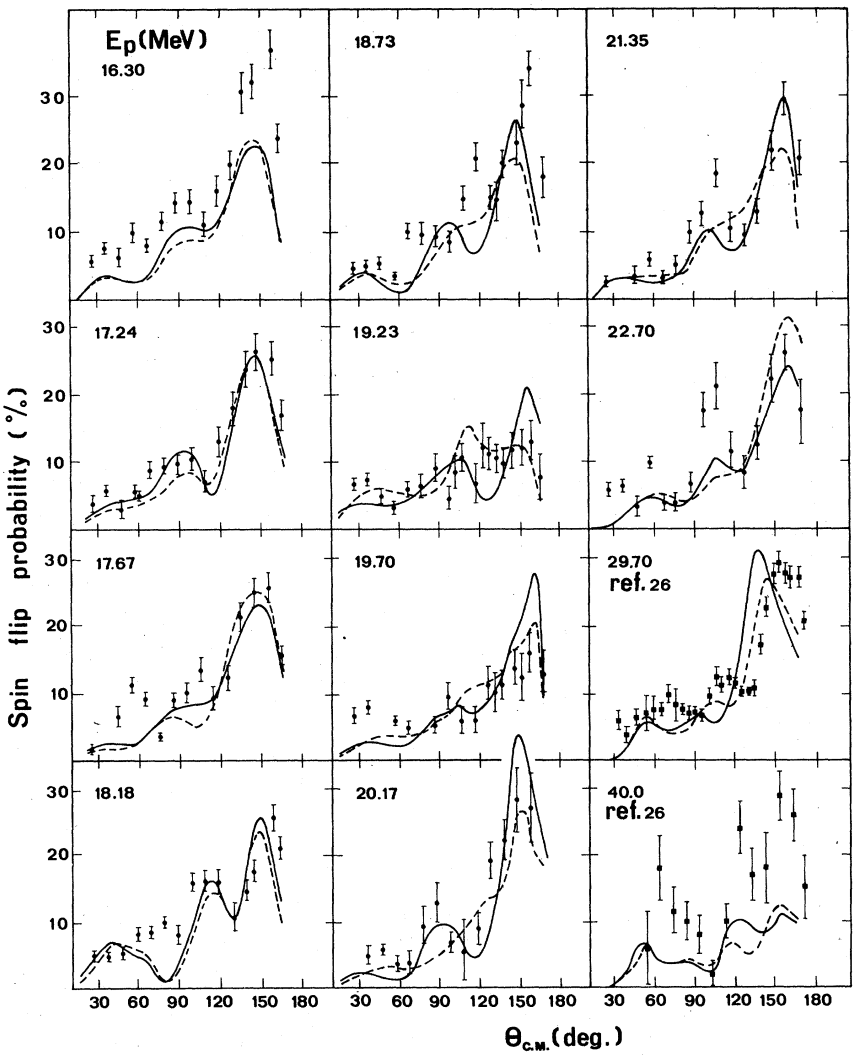

FIG. 11. As Fig. 9 for the angular distributions of the SFP relative to the inelastic proton scattering from the 2^+ state of ^{28}Si.

(EWSR) which, for isoscalar transitions exhausting all the EWSR, in $N=Z$ nuclei, impose the condition

$$\beta_L^2 = L(L+1)\frac{\hbar^2}{2mR^2}\frac{4\pi}{3A}\frac{1}{\hbar w_L}$$

$$= 87L(L+1)R^{-1}(A\hbar w_L)^{-1} \qquad (6.3)$$

and for isovector dipole excitation

$$\beta_L^2 = 1044(1+0.8x)R^{-2}(A\hbar w_L)^{-1}. \qquad (6.4)$$

The meaning of x may be deduced from Ref. 33. It is, however, equal to zero for the $Z<20$ nuclei.

For most of the nuclei, the GR strength distributions are not well known yet. Thus together with their relative phases $\phi_\lambda(\bar{Q})$, they are treated as adjustable parameters in a search process for fitting data. Generally a small number of terms is retained and where possible the strengths are constrained to the EWSR restriction and to the energy positions chosen following the GR known mass-energy variation.[33]

To deduce the normalization factor of the spin-orbit strength V_{LS} several tests have been performed. The 0.5 value has been used by Eikemaier and Hackenbroich[31] and 0.25 by Shaffer and Raynal.[34] In Fig. 8 the direct reaction part of the calculations performed with these two values is compared with experimental data at 40.0 MeV. Curves with $V_{LS}=0.5$ are in good agreement with all the spin-dependent data while they exceed the 2^+ cross section; an inverse agreement occurs using $V_{LS}=0.25$. In order to fit at the same time all the 2^+ data available, the value 0.35 has been chosen for this level, while the 0.5 one has been used for the 3^+

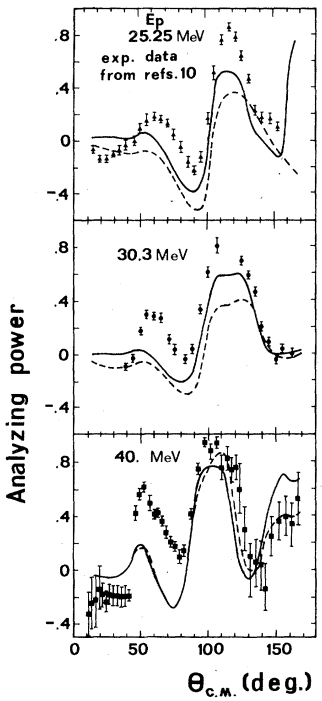

FIG. 12. As Fig. 9 for the angular distributions of the analyzing powers relative to the inelastic proton scattering from the 2^+ state of ^{28}Si.

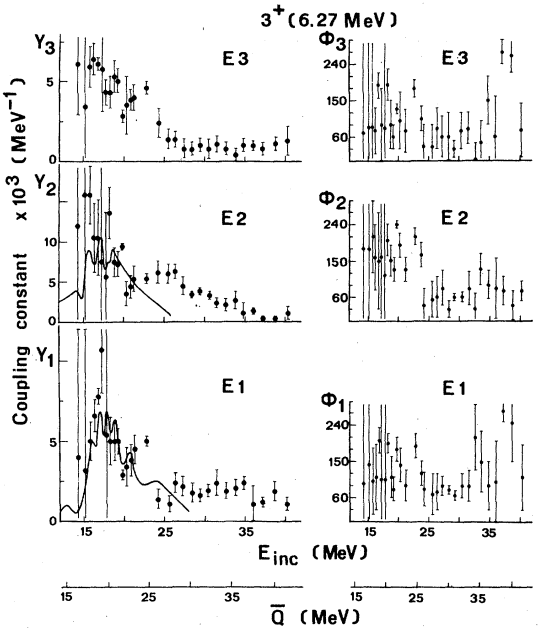

FIG. 14. Variation with the incident (E_p) and excitation ($\bar{Q}$) energies of the core exchange $\lambda=1,2,3$ complex coupling constants determined fitting the experimental data in Fig. 10. The full lines on $Y1$ and $Y2$ represent, respectively, the dipolar and all the isoscalar GR strengths.

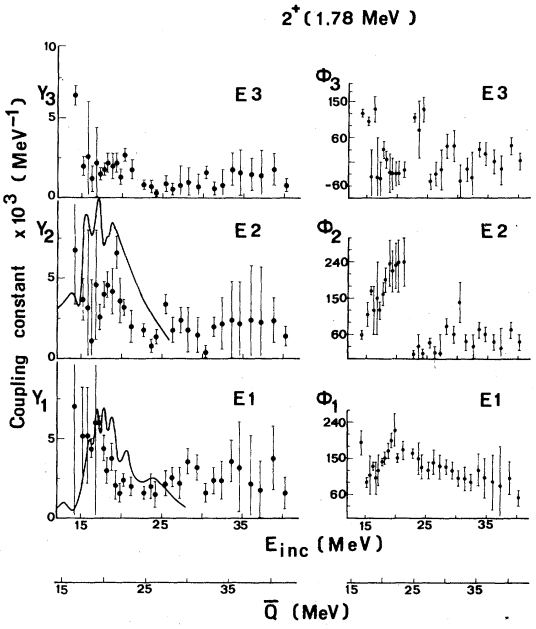

FIG. 13. Variation with the incident (E_p) and excitation ($\bar{Q}$) energies of the core exchange $\lambda=1,2,3$ complex coupling constants determined fitting the experimental data in Figs. 9, 11, and 12. The full lines on $Y1$ and $Y2$ represent, respectively, the dipolar and all the isoscalar GR strengths.

cross sections. So the V_{LS} has been treated as an effective level dependent interaction.

At 40.0 MeV the agreement for the 2^+ cross section is good (see Fig. 8); this denotes the validity of the spectroscopy assumed. The agreement, however, is poor for spin-dependent data in the same way as it is in macroscopic calculations. The ratio between the 2^+ integrated experimental and the direct microscopic cross sections thus evaluated, remains constant and nearly one above 20 MeV; it increases to 1.5 at lower energies, reproducing the energy dependence of β_2 found in macroscopic analysis. For the 3^+ transition the same ratio is highly energy dependent and increases from the value of 1.3 at 40 MeV to the one of 57 at 15.3 MeV; so nondirect contributions are important to fit, in all the energy range, the shapes and the absolute values of the 3^+ cross sections.

Two complete microscopic calculations, including resonance contributions, have been performed on each level. The first calculation searched for the dipolar and the quadrupolar complex coupling constants $M(\bar{Q})$; in the second calculation the search was extended to the octupolar resonance. The inclusion of the hexadecapole resonance was tested, but no noticeable improvement of the fits was noted.

Figures 9–12 contain the fits both for the two

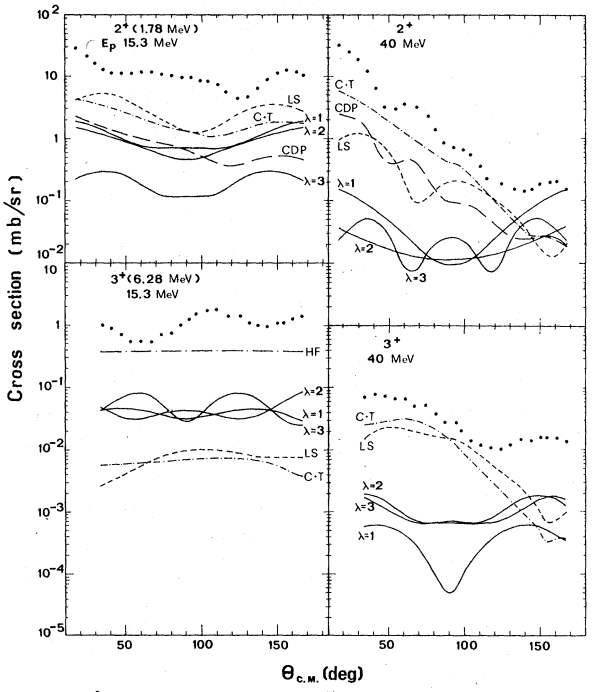

FIG. 15. Central and tensor (C+T) valence, LS valence (LS), core direct polarization (CDP) and core exchange ($\lambda=1,2,3$) contributions to the microscopic ADWBA calculations shown in Figs. 10 and 11 related to the 2^+ and 3^+ cross sections, at $E_p=15.3$ and 40.2 MeV (points). The core exchange contributions have been arbitrarily normalized. The CN contribution (HF) for the 3^+ cross section at $E_p=15.3$ MeV is also shown.

(dashed lines) and for the three (full lines) resonance searches, whereas Figs. 13–14 show the complex coupling constants found in the second analysis. The different reaction mechanism contributions to the 2^+ and 3^+ cross sections are shown at two energies in Fig. 15.

Between 30 and 40 MeV the strength distributions in Figs. 13–14 appear small and smoothly decreasing but, at the lowest measured energies they show no clear-cut decrease. Moreover the strengths in Figs. 13–14 are similar both in shape and in magnitude, denoting the independence of the obtained information upon the excited level from which scattering is observed. The curves drawn on $E1$ and $E2$ points in Figs. 13–14 represent, respectively, the isovector dipolar GR as deduced from photonuclear reactions,[35] and the contributions of all isoscalar GR with a dominant quadrupolar term, extracted from the nuclear continuum of a ^{28}Si(α, α') reaction.[8] The agreement between the two curves and the deduced points proves that virtual excited intermediate levels represent GR states of ^{28}Si.

In the present analysis the coupling constant phase errors are large, thus hindering GR transition strength β_λ deductions through the equation[36]

$$\mathrm{Im}\int_{-\infty}^{\infty} M_\lambda(\bar{Q})d\bar{Q}=\pi\beta_\lambda^2/(2\lambda+1)\,. \tag{6.5}$$

However, a rough estimate of the EWSR fraction present in the GR states may be performed using the method reported by Perrin *et al.*[36] which supposes the strength distributions formed by several discrete resonances each with its own position, strength, and width. Assuming a uniform mass distribution in the ^{28}Si, 20% of the EWSR is found in the $E1$ strengths and 40% in the $E3$, presumed to be all isoscalar in character. The $E2$ exhausts all the isoscalar EWSR limit; therefore, also in consequence of the $\phi_2(\bar{Q})$ behavior which is split in two separated branches in all the searches, the existence of an isovector quadrupolar GR contribution may be hypothesized.

The EWSR percentages reported are affected by great uncertainty since they strongly depend upon fit procedure, spectroscopy uncertainty, and the model used to evaluate the direct contribution.

VII. CONCLUSIONS

The study of proton scattering from low-lying states of ^{28}Si in the 14–40 MeV range cannot be correctly interpreted only by a pure one-step direct reaction mechanism.

The CC method can describe the $0^+, 2^+, 4^+, 3^-$ cross section absolute values, but it cannot always account for their angular shapes. The transition strengths, moreover, must be thought of as energy dependent and greatly increased at low energies; SFP result largely not fitted.

A microscopic DWBA calculation fails to account for all spin-dependent data. This is more evident for the 3^+ cross sections at low energies where experimental points exceed the calculated values by at least one order of magnitude.

To explain these failures we have added components due to two-step processes via GR intermediate states in the reaction mechanism, and in this way, we have fully interpreted the 2^+ and 3^+ level data.

The ^{28}Si $E1$, $E2$, and $E3$ GR strength distributions have been deduced treating the coupling strengths of the intermediate states as free parameters. The GR information extracted has been shown to be essentially nondependent upon the inelastic channel investigated and in good agreement with the results from photonuclear and α inelastic scattering reactions.

A comparison between Figs. 5 and 11 shows the most significant result of this work: the resonance

contribution makes a large qualitative difference in the SFP calculations and greatly improves their agreement with experiment. The resonant contribution is essential to explain the SFP and the 3^+ cross sections; otherwise it is of minor importance.

We acknowledge Mr. P. Tempesta, Dr. M. Tarantino and the staff of the cyclotron of Milan for technical support.

---

*Now at B. C. M. N., Geel-Belgium.
[1]H. V. Geramb, R. Sprickmann, and G. L. Strobel, Nucl. Phys. A199, 545 (1973).
[2]C. R. Lamontage, B. Frois, R. J. Slobodrian, H. E. Conzett, C. Leemann, and R. de Swiniarski, Phys. Lett. 45B, 465 (1973).
[3]H. R. Weller and M. Divadeenam, Phys. Lett. 55B, 41 (1975).
[4]H. V. Geramb, K. Amos, R. Sprickmann, K. T. Knöpfle, M. Rogge, D. Ingham, and C. Mayer-Böricke, Phys. Rev. C 12, 1697 (1975).
[5]R. De Leo, G. D'Erasmo, F. Ferrero, A. Panteleo, and M. Pignanelli, Nucl. Phys. A254, 156 (1975).
[6]L. Lovas, M. Rogge, V. Schwinn, P. Turek, D. Ingham, and C. Mayer-Böricke, Nucl. Phys. A268, 12 (1977).
[7]N. Bezic, D. Jamnik, G. Kernel, J. Krajnik, and J. Snajder, Nucl. Phys. A117, 124 (1968).
[8]K. T. Knöpfle, G. R. Wagner, A. Kiss, M. Rogge, C. Mayer-Böricke, and T. Bauer, Phys. Lett. 64B, 263 (1976); K. Van der Borg, M. N. Harakeh, S. Y. Van der Werf, A. Van der Woude, and F. E. Bertrand, *ibid.* 67B, 405 (1977).
[9]R. Sprickmann, K. T. Knöpfle, D. Ingham, M. Rogge, C. Mayer-Boricke, and H. V. Geramb, Z. Phys. A274, 339 (1975).
[10]A. G. Blair, C. Glashausser, R. de Swiniarski, J. Goudergues, R. Lombard, B. Mayer, J. Thirion, and P. Vaganov, Phys. Rev. C 1, 444 (1970); R. de Swiniarski, H. E. Conzett, C. R. Lamontage, B. Frois, and R. J. Slobodrian, Can. J. Phys. 51, 1293 (1973); R. de Swiniarski, F. G. Resmini, D. L. Hendric, and A. D. Backer, Nucl. Phys. A261, 111 (1976); M. P. Fricke, R. M. Drisko, R. H. Bassel, E. E. Gross, B. J. Morton, and A. Zucher, Phys. Rev. Lett. 16, 746 (1966).
[11]M. A. Melkanoff, J. Raynal, and T. Sawada, Report No. UCLA 68-10, 1966 (unpublished).
[12]E. Colombo, R. De Leo, J. L. Escudié, S. Micheletti, M. Pignanelli, and F. G. Resmini, in *Proceedings of the International Conference on Nuclear Structure, Tokyo, 1977*, edited by T. Marumori (Physical Society of Japan, Tokyo, 1978), p. 490.
[13]F. D. Becchetti and J. W. Greenlees, Phys. Rev. 182, 1190 (1969).
[14]K. W. Kemper, J. D. Fox, and D. W. Oliver, Phys. Rev. C 5, 1257 (1972); G. D. Gunn, K. W. Kemper, and J. D. Fox, Nucl. Phys. A232, 176 (1974).
[15]A. C. Shotter, P. S. Fisher, and D. K. Scott, Nucl. Phys. A159, 577 (1970).
[16]T. Ericson, Adv. Phys. 9, 425 (1960).
[17]H. Feshbach, in *Nuclear Spectroscopy*, edited by F. Ajzenberg-Selove (Academic, New York, 1960).
[18]J. R. Huizenga and G. Igo, Nucl. Phys. 29, 462 (1962); J. M. Lohr and W. Haeberli, *ibid.* A232, 381 (1974); D. Wilmore and P. E. Hodgson, *ibid.* 55, 673 (1964).
[19]C. M. Perey and F. G. Perey, At. Data Nucl. Data Tables 17, 1 (1976).
[20]A. L. Goodman, G. L. Struble, J. Bar-Tour, and A. Goswami, Phys. Rev. C 2, 380 (1970).
[21]K. J. Le Couteur and D. W. Lang, Nucl. Phys. 13, 32 (1959); W. Dilg, W. Schantl, H. Vonach, and M. Uhl, Nucl. Phys. A217, 269 (1973).
[22]E. Gadioli and Z. Zetta, Phys. Rev. 167, 1016 (1968).
[23]A. G. W. Cameron, Can. J. Phys. 36, 1040 (1958).
[24]J. Raynal, private communication.
[25]H. Sherif, Nucl. Phys. A131, 532 (1969).
[26]R. O. Ginaven, E. E. Gross, J. J. Malinify, and A. Zucker, Phys. Rev. Lett. 21, 552 (1968).
[27]H. Rebel, G. W. Schweimer, G. Schatz, J. Specht, R. Loken, G. Hauser, D. Habs, and H. Klewe-Nebenius, Nucl. Phys. A182, 145 (1972).
[28]A. De Shalit and I. Talmi, *Nuclear Shell Theory* (Academic, New York and London, 1963).
[29]H. Wildenthal, private communication.
[30]S. M. Austin, *Two Body Force in Nuclei* (Plenum, New York, 1972).
[31]H. Eikemaier and H. H. Hackenbroich, Nucl. Phys. A169, 407 (1971).
[32]W. G. Love and G. R. Satchler, Nucl. Phys. A172, 449 (1971); A101, 424 (1967).
[33]G. R. Satchler, Nucl. Phys. A195, 1 (1972); Phys. Rep. 14C, 98 (1974).
[34]R. Schaeffer and J. Raynal, private communication.
[35]A. Veyssiere, H. Beil, R. Bergere, P. Carlos, A. Leprêtre, and A. De Miniac, Nucl. Phys. A227, 427 (1974).
[36]G. Perrin, D. Lebrun, J. Chauvin, P. De Santignon, D. Eppel, H. V. Geramb, H. L. Yadav, and V. A. Madsen, Phys. Lett. 68B, 55 (1977).